

# A Mechanochemical Switch to Control Radical Intermediates

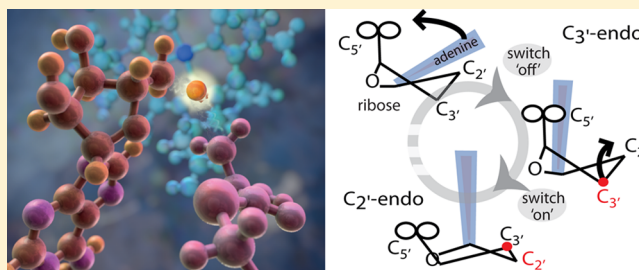
Elizabeth Brunk,<sup>†</sup> Whitney F. Kellett,<sup>‡</sup> Nigel G. J. Richards,<sup>‡</sup> and Ursula Rothlisberger<sup>\*,†</sup>

<sup>†</sup>Laboratory of Computational Chemistry and Biochemistry, EPFL, Lausanne, Switzerland 1015

<sup>‡</sup>Indiana University-Purdue University, Indianapolis, Indiana 46202, United States

## S Supporting Information

**ABSTRACT:** B<sub>12</sub>-dependent enzymes employ radical species with exceptional prowess to catalyze some of the most chemically challenging, thermodynamically unfavorable reactions. However, dealing with highly reactive intermediates is an extremely demanding task, requiring sophisticated control strategies to prevent unwanted side reactions. Using hybrid quantum mechanical/molecular mechanical simulations, we follow the full catalytic cycle of an AdoB<sub>12</sub>-dependent enzyme and present the details of a mechanism that utilizes a highly effective mechanochemical switch. When the switch is “off”, the 5′-deoxyadenosyl radical moiety is stabilized by releasing the internal strain of an enzyme-imposed conformation. Turning the switch “on,” the enzyme environment becomes the driving force to impose a distinct conformation of the 5′-deoxyadenosyl radical to avoid deleterious radical transfer. This mechanochemical switch illustrates the elaborate way in which enzymes attain selectivity of extremely chemically challenging reactions.



Enzyme regulation is not only about facilitating target reactions but also about preventing those that are undesired. The idea that enzymes lower the activation energy of a chemical transformation is central to the understanding of how enzymes catalyze reactions at astounding rates, relative to the uncatalyzed process in solution. However, reactions that involve highly reactive and unstable intermediates, such as a radical species, present an entirely new set of catalytic challenges. Under these circumstances, the challenge of attaining reaction selectivity requires stabilizing and prolonging the lifetime of the reactive intermediates to ensure proper product formation. For this task, it has been suggested that certain enzymes resort to using a tactic that prevents reactive intermediates from undergoing spontaneous and erroneous side reactions in an effort to stabilize themselves.<sup>1</sup> Potentially threatening side reactions can encumber specificity by competing with the native radical transfer mechanism by having lower kinetic barriers and forming products that are more stable.

Naturally, the long list of complications that could potentially annihilate radical chemistry raises the question: what is the payoff in dealing with such highly reactive species? In the case of vitamin B<sub>12</sub>, nature has found an elegant way to employ a radical species with exceptional prowess in order to catalyze some of the most chemically challenging, thermodynamically unfavorable reactions. For 5′-deoxyadenosyl-cobalamin (AdoCbl) dependent isomerases, homolysis of the carbon–cobalt bond (Co–C), the so-called “radical reservoir”,<sup>2</sup> generates a highly reactive, primary carbon radical species (designated Ado• in Figure 1a), which has the capability of abstracting a primary hydrogen atom from an unactivated carbon atom of the substrate. Thus, accomplishing the feat of

Co–C bond homolysis provides a very useful tool for enzymes to meet the demands of particularly challenging chemical tasks, such as, in the case of methyl malonyl-CoA mutase (MCM) and glutamate mutase (GM), carbon skeleton rearrangements.

However, enzymes pay a high price to make use of the potency of such a radical reservoir. The cost of using this tool is manifested in two ways: (i) the energy required to form the radical intermediate and (ii) the energy required to control it. For the first point, breaking the Co–C bond requires overcoming an energetic barrier of  $31.0 \pm 1.5$  kcal mol<sup>−1</sup> in solution<sup>3</sup> or 15–17 kcal mol<sup>−1</sup> in an enzyme environment.<sup>4</sup> It has been suggested that AdoCbl bond labilization may, in part, be achieved by steric crowding, through local interactions with the 5′-deoxyadenosyl radical moiety, angular distortions in the corrinoid ring, or encumbrance by an active site residue.<sup>5</sup> Additionally, substrate-induced, large-scale domain motions appear to be coupled to the activation of the AdoCbl bond in certain AdoCbl-dependent enzymes.<sup>6</sup> However, once homolysis has been accomplished, the enzyme’s work is not yet finished; the radical site must be transferred to the substrate to initiate the rearrangement reaction. To this end, migration of Ado• takes place over several angstroms,<sup>7,8</sup> in certain cases as far as 10 Å from its original position,<sup>9</sup> proximal to co(II)balamin. This leads to the second point: stabilizing Ado• during this translocation is of the utmost importance to ensure that the radical reacts with the proper atom on the substrate for the desired transformation.

Received: January 13, 2014

Revised: May 17, 2014

Published: May 20, 2014

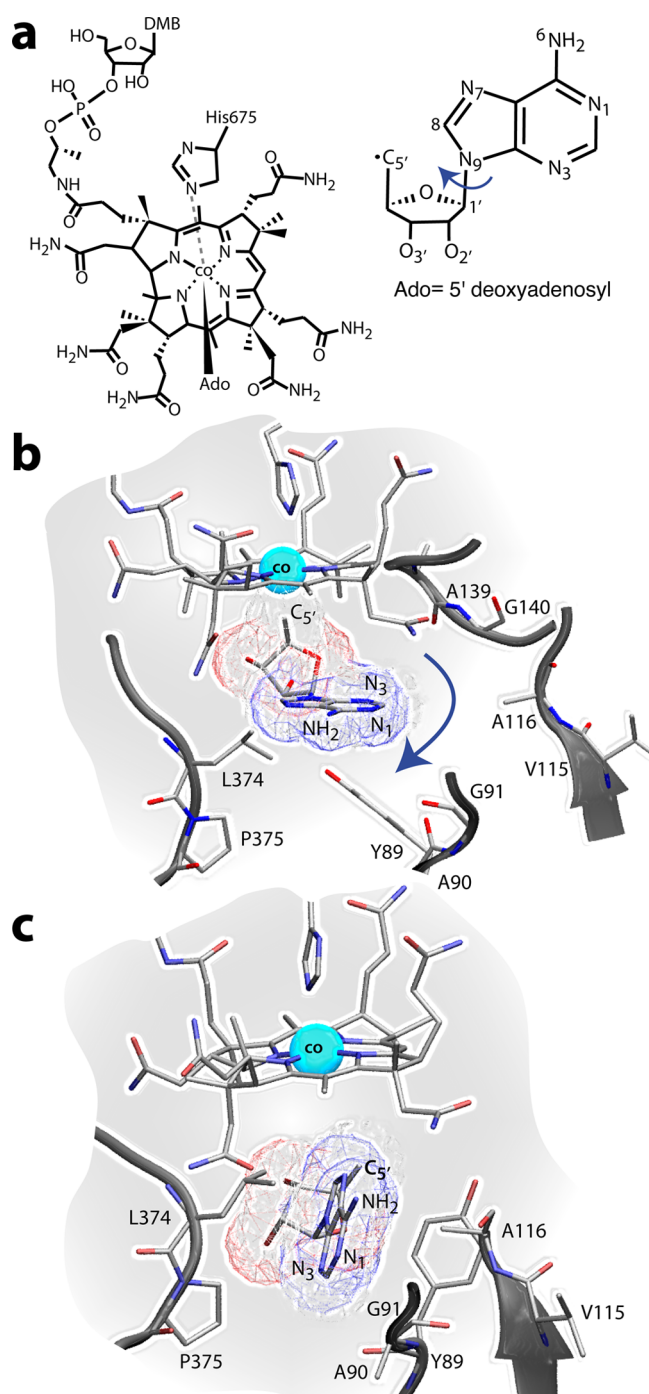


**Figure 1.** Adenosylcobalamin cofactor. In (a), the B<sub>12</sub> cofactor, doubly coordinated with a histidine residue (DMB-off conformation) and the 5'-deoxyadenosyl moiety (Ado). In (b) and (c), the crystal structures of bound (pdb entry 3REQ) and unbound Ado (pdb entry 4REQ), respectively, demonstrate the change in conformation of the adenine base relative to the B<sub>12</sub> corrinoid ring.

To avoid factors that jeopardize selectivity, a radical intermediate must be protected predominantly from potential threats of the solvent, the protein environment, and itself. Protection from these agents may take place in the form of sequestration from groups that might react with it and/or steric tuning to avoid conformations from which undesired reactions are likely to occur. It has been suggested that protection of the radical species from solvent is achieved through a common

architecture, found in numerous AdoCbl-dependent enzymes, that is, the ( $\beta/\alpha$ )<sub>8</sub>-TIM-barrel structural motif. This fold is typically characterized by a central barrel formed by parallel beta-strands surrounded by seven or eight alpha helices, which isolates the highly reactive radical species in a deep hydrophobic cleft at the center of the protein, reducing the occurrence of unwanted side reactions with solvent. However, an equally important task requires the enzyme to assume strict control over the radical intermediates *themselves*, to suppress side reactions and protect the interior of the protein from damage.

Understanding how AdoCbl-dependent enzymes control and manipulate transient radical species with high fidelity is a subject that has received less attention when compared to other aspects of the catalytic reaction, such as the origin of the  $>10^{10}$ -fold rate enhancement of Co–C bond homolysis or the extent to which homolysis is coupled to hydrogen abstraction. Nevertheless, various contributions from both experiment<sup>5,10–12</sup> and computation<sup>13–17,19</sup> have provided valuable insights that help to better understand the elusive nature of the 5'-deoxyadenosyl radical moiety (for a review, see ref 20) and its journey to the substrate. Of relevance to these issues are studies that describe various conformations of Ado• that may be important to catalysis as well as the roles of nearby amino acids with which it may interact. For example, potentially important conformational changes include a pseudorotation of the glycosyl moiety, reported in diol dehydratase,<sup>7</sup> a puckering of the ribose moiety, seen in GM,<sup>8</sup> and an adenine-ribose rotation about the glycosidic bond in MCM.<sup>13,21</sup> Previous theoretical studies on certain conformational changes in the adenosyl moiety, such as ribose puckering, attribute the changes in geometry to strain induced from the bound configuration.<sup>6</sup> Other findings from the crystallographic structure<sup>22</sup> of MCM suggest that Ado• adopts the *syn* conformation (in the Pullman notation<sup>23</sup>), when bound to cobalamin and the *anti* conformation, when the AdoCbl bond has ruptured.<sup>13</sup> Consistent with this finding is the 8,5'-cyclic structure,<sup>24</sup> formed via the intramolecular interactions of the C5' atom with position 8 of adenine. This conformation was inferred from previous experiments of tritium labeled H<sub>2</sub>O which exchanges with the H<sub>8</sub> atom of adenosine<sup>25</sup> (see Figure 1a), whereas stabilizing intermolecular interactions may involve co(II)-balamin,<sup>26</sup> acting as the “conductor” to lower the transition-state energy barrier for radical formation and rearrangement, B<sub>12</sub>:C19–H, interacting with the O<sub>3'</sub> of the ribose moiety of Ado•,<sup>27,28</sup> or a conserved glutamate residue (E370 in MCM,<sup>29</sup> E330 in GM,<sup>8</sup> and E338 in ornithine 4,5-aminomutase (OAM)<sup>30</sup>).

However, despite the many valuable contributions, piecing the various findings together to formulate a clear picture that establishes the key factors responsible for reaction selectivity of the radical intermediates has not been possible. Ultimately, utilizing the AdoCbl cofactor requires finding a delicate balance between stabilizing Ado• while still preserving its reactive nature. Missing from the current understanding are the inner workings of the enzymatic reaction mechanism that achieve such a balance, and, in particular the role the enzyme environment plays in asserting strict control over Ado• during catalysis. In particular, understanding how and why the enzyme manipulates conformations of Ado• during the catalytic cycle as a possible mechanism to ensure selectivity deserves further attention. This contribution addresses not only the initial generation of the radical species but especially the further fate

of the 5'-deoxyadenosyl radical moiety throughout its journey prior to hydrogen abstraction from the substrate. Studying the catalytic mechanism of MCM, we find that the enzyme acts as a mechanochemical switch to manage conformational changes in Ado $\cdot$  by imposing or releasing strain at distinct stages of the catalytic cycle to effectively channel the reaction in a desired direction. Interestingly, this switch can either be deactivated through homolysis or activated through intermolecular interactions between the 5'-deoxyadenosyl radical moiety and the protein. Using key conformational changes of Ado $\cdot$  as a transformational trigger suggests that such a mechanism may be inherent in other AdoCbl-dependent enzymes.

## ■ COMPUTATIONAL METHODS

All classical molecular dynamics (MD) simulations were carried out using the AMBER suite of programs.<sup>31</sup> Starting from a model made from two crystal structures of MCM (pdb entries 1E1C and 3REQ), modifications, such as the mutation A244H, were made to recover the wild-type sequence of MCM. Nonstandard residues (B<sub>12</sub>, Ado, His610 and the substrate, methyl malonyl-CoA and lactoyl-CoA) were parametrized using the AMBER 99sb force field<sup>32</sup> by following the modeling of cobalt corrinoids from previous studies.<sup>33</sup> The particle mesh Ewald (PME) method, with a nonbonded cutoff of 12 Å, was used with periodic boundary conditions and the Langevin piston Nosé–Hoover method<sup>34,35</sup> to ensure constant pressure and temperature conditions. Classical MD trajectories were performed for 100 ns before the structures were used to initialize the QM/MM simulations. For the QM/MM simulations, we used an extension of Car–Parrinello molecular dynamics (CPMD 3.13)<sup>36,37</sup> to run Born–Oppenheimer molecular dynamics (BOMD) using a time step of 10 au and a fictitious electron mass of 400 au. We described the QM atoms by the DFT/BLYP functional<sup>38,39</sup> and norm-conserving Martins–Trouiller pseudopotentials<sup>40</sup> with dispersion-corrected atom-centered potentials.<sup>41</sup> The accuracy of BLYP to describe the structural and electronic properties of cobalamins has been previously reported.<sup>42</sup> Moreover, the electronic structure and mechanism of cobalamin and adenosylcobalamin-dependent enzymes has been extensively studied using similar methods.<sup>43–45</sup> We included 123 atoms in the QM subset, which consists of the coordinating histidine residue (H610), capped with a monovalent pseudopotential<sup>46</sup> at the beta carbon, the entire 5'-deoxyadenosyl radical moiety (Ado), the cobalt corrin ring, capped at the COMe and NHMe side chains, and the substrate, in which the CoA tail has been capped at the second carbon after the sulfur atom. The wave functions were expanded in a plane wave basis set with a 70 Ry cutoff inside a orthorhombic quantum box with dimensions 23.2 × 29.5 × 21.6 Å<sup>3</sup>. This cutoff has been shown to achieve a good convergence of energies and structural properties of cobalt complexes in previous studies on vitamin B<sub>12</sub>.<sup>45,47</sup> In addition, we found that increasing the cutoff to 95 Ry does not result in significant changes in relative energy (see Supporting Information). Long-range interactions of the QM part were decoupled using the Martyna–Tuckerman scheme.<sup>48</sup> The MM subset was characterized by a classical AMBER 99sb force field and contained the rest of the protein and explicit solvent water molecules and 20 Na<sup>+</sup> counterions for system neutrality. The QM/MM simulations were performed at constant pressure and temperature, using the Nosé–Hoover thermostat. The system was equilibrated for 20 ps before performing thermodynamic integration.<sup>49</sup> Using constrained BOMD, the reaction coordinate

was fixed in increments of 0.1 Å from 2.1 to 3.6 Å to cleave the Co–C bond over a period of 30 ps. Upon cleavage of the Co–C bond, the system was further equilibrated for 15 ps before the hydrogen abstraction reaction took place, using a similar protocol. The second step is characterized by a reaction coordinate that describes the distance between the C<sub>5'</sub> atom on Ado $\cdot$  and the primary hydrogen atom on the substrate, spanning distances of 4–1.1 Å in increments of 0.1 Å. Another reaction coordinate used to characterize hydrogen abstraction was the distance between the C5' atom of adenosyl and the tertiary hydrogen on the subsequent carbon atom (H<sub>3'</sub>). Additionally, we explored the rotation of the adenine base about the glycosidic bond ( $\phi$  = O<sub>4'</sub>–C<sub>1'</sub>–N<sub>9</sub>–C<sub>8</sub>, Figure 1b), increasing the reaction coordinate ( $\phi$ ) from ~50 to 100° in five windows with increments of ~10°. Hysteresis was evaluated by performing the back reaction for both homolysis and abstraction steps. Gas phase calculations were performed using Gaussian '09 (G09).<sup>50</sup> Optimizations and relaxed scans were performed at different levels of theory, including DFT and MP2 and with various basis sets.<sup>51</sup> For more details see the Supplementary Methods.

## ■ PREPARATION OF MCM ACTIVE ENZYME

*Propionibacterium shermanii* mutB and mutA genes which code for the  $\alpha$  subunit and  $\beta$  subunit, respectively, were codon-optimized for expression in *Escherichia coli* and synthesized using standard algorithms (Life Technologies/Thermo Scientific/Fisher). The genes were ligated into pETDuet-1 (Novagen) and with an N-terminal His-tag on the mutA product. Purified and sequenced construct was transformed into BL21 DE3 chemically competent cells and expressed using approaches from previous standard procedures<sup>52,53</sup> with minor alterations, such as the addition of a 10 min, 42 °C heat shock step prior to induction. The cells were pelleted and lysed using known procedures, except that an additional cell lysis step was performed on the initially retrieved cell pellet. Appreciable amounts of soluble protein were detected in both cell lysate solutions (from first and second pelleting), and thus the lysate was pooled and exchanged with dialysis into 50 mM potassium phosphate buffer, pH 7.5, overnight at 4 °C. The protein was purified with 6x-His affinity Ni(II) binding resin (Qiagen, Hilden, Germany). Protein was then reconstituted overnight with 5'-deoxyadenosyl-cobalamin (Sigma-Aldrich, St. Louis, MO) under reduced ambient light. Excess cofactor was removed with a P-30 spin column (BioRad, Hercules, CA).

## ■ ASSAY OF MCM ACTIVITY

MCM was assayed by Accurate-Mass Q-TOF LC/MS (Agilent) using adaptations of published methods to analyze the presence of CoA esters. Purified protein (5  $\mu$ g), previously reconstituted with cofactor, was inoculated with substrate (methylmalonyl-CoA, 0.1 mg) and run for several time points as well as overnight at 37 °C and in the dark. Ten microliters of each reaction was injected for analysis, and the mass spectrometry peaks for methylmalonyl-CoA were integrated and analyzed against a standard curve constructed of five different substrate concentrations (software Agilent Mass Hunter Acquisition and Q-TOF Quantitative Analysis). For more details, see the Supporting Information.



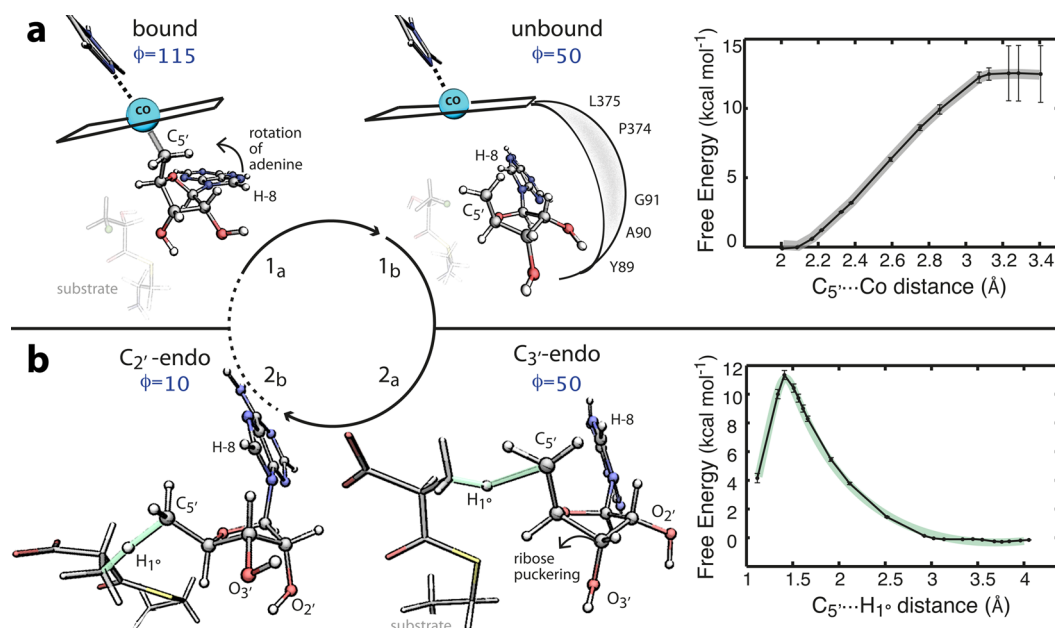


**Figure 2.** Mechanochemical switch. Upon homolysis, illustrated by the stages 1<sub>a</sub> to 1<sub>b</sub>, Ado<sup>•</sup> diffuses out of its cavity and undergoes a spontaneous conformational change in which the adenine base rotates by 100° to an orientation perpendicular to the corrinoid ring. The hydrophobic and nonpolar residues lining the cavity around the adenine base allow for this rotation to be diffusion controlled. The panel on the upper right displays the free energy profile for  $\text{Co}\cdots\text{C}_5'$  bond cleavage. In contrast, during the hydrogen abstraction reaction, illustrated by the stages 2<sub>a</sub> to 2<sub>b</sub>, the enzyme mediates the conformational change in Ado<sup>•</sup> from  $\text{C}_3'$ -endo to  $\text{C}_2'$ -endo via nearby charged and polar residues which exchange hydrogen bonds with axial  $\text{O}_3'$  and equatorial  $\text{O}_3$ . The panel on the lower right displays the free energy profile for hydrogen abstraction. The maximum error obtained along the profiles are indicated by the error bars.

## RESULTS AND DISCUSSION

### Conformational Changes That Accompany Cleavage.

Homolysis demands the scission of the kinetically inert AdoCbl bond to initiate radical chemistry. One of the main challenges at this step in the catalytic cycle is to prevent recombination from occurring in order to transfer the radical to the substrate. To probe the functional relationship between cofactor, enzyme and substrate during the homolytic cleavage reaction, we studied the catalytic cycle of MCM using both classical and quantum mechanical/molecular mechanical (QM/MM) Car–Parrinello<sup>37</sup> molecular dynamics (CPMD) simulations.

The choice of starting structure for the classical MD simulations was selected to embody the characteristics of the AdoCbl cofactor before homolysis. Various crystallographic structures of MCM reveal different orientations of the 5'-deoxyadenosyl radical moiety, which appear to differ based on whether the Co–C bond is formed or broken. When AdoCbl is in the bound state ( $\text{Co}–\text{C} < 2.5$  Å), such as for pdb entry 3REQ,<sup>12</sup> the enzyme is referred to as the open and unreactive state, and the conformation of the adenine ring is said to be *syn*.<sup>13</sup> In this state, the adenosine base is in a position that is parallel to the corrinoid ring, typically constrained by two side chains of the B<sub>12</sub> pyrrole ring B. Characteristic of this conformation is a value for the glycosidic dihedral angle ( $\phi = \text{O}_4–\text{C}_1–\text{N}_9–\text{C}_8$ , Figure 1b) greater than  $\sim 90^\circ$ . In contrast, in the unbound state of AdoCbl ( $\text{Co}–\text{C} > 3.5$  Å), such as for pdb entries 4REQ<sup>12</sup> and 2XIQ,<sup>54</sup> Ado<sup>•</sup> adopts the *anti* conformation in which the adenosine base is perpendicular to the corrin ring (Figure 1c and Supplementary Figure 1, Supporting Information). The value of  $\phi$  in this conformation is in the range of 45–55°. These distinct conformations of Ado<sup>•</sup> are consistently observed in crystallographic structures of other AdoCbl-dependent enzymes (Supplementary Table 1, Supporting

Information), such as GM (pdb entry 1I9C<sup>8</sup>) and OAM (pdb entry 3KOZ<sup>55</sup>).

It has been previously suggested that the AdoCbl-dependent proteins undergo large-scale conformational rearrangements upon binding to the substrate,<sup>19</sup> which signals the importance of selecting a starting structure in complex with a substrate. Taking these observations into consideration, we began the MD simulations using a structure in the closed (reactive) state and with an intact AdoCbl bond. Insertion of the 5'-deoxyadenosyl moiety from 3REQ into pdb entry 1E1C<sup>22</sup> gave a model with MCM in the closed state (in complex with a desulfo coenzyme A ester, in which the terminal acyl and sulfur groups have been removed) and a final representation of AdoCbl in a “base-off”, hexa-coordinated, “bound” co(III)-balamin state (a Co–C bond length of 2.1 Å) with the adenosyl group in the *syn* conformation and the ribose moiety adopting a  $\text{C}_3'$ -endo conformation. Our QM/MM model shows good agreement with the open (reactive) state of the enzyme, and a comparison can be found online in Supplementary Figure 2 and Supplementary Table 2, Supporting Information. Starting the QM/MM simulations from the classically equilibrated structure, we chose to describe homolytic cleavage with the  $\text{C}_5'\cdots\text{Co}$  distance as the designated reaction coordinate. The free energy barrier determined from thermodynamic integration<sup>49</sup> (TI) was  $12.4 \pm 1.9$  kcal mol<sup>-1</sup>, in good agreement with estimates from kinetic experiments as well as computational simulations (13.1–15.3 kcal mol<sup>-1</sup>).<sup>6,10,14,15</sup>

Cleavage of the glycosidic bond induces a significant molecular event as a result of the formation of the radical intermediate, Ado<sup>•</sup>. After removing the constraint on the reaction coordinate at 3.6 Å, Ado<sup>•</sup> diffuses 3 Å from its original binding position, out of the cavity proximal to the B<sub>12</sub> pyrrole ring B. This relieves the adenosine base from a previous, sterically confined configuration (*syn*) and allows for its

rotation of nearly  $100^\circ$  about the glycosidic bond (Supplementary Video 1, Supporting Information and Figure 3), which orients the base orthogonal to the corrinoid ring (1a versus 1b in Figure 2). Our findings indicate that Ado $\cdot$  adopts this *anti*

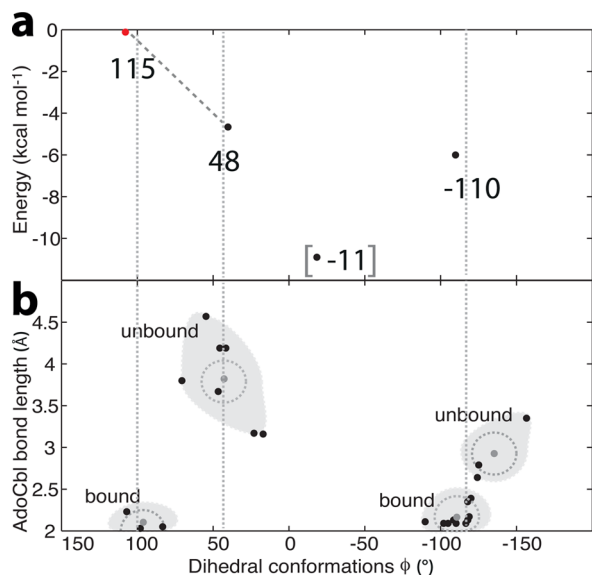


**Figure 3.** Different conformations of Ado $\cdot$  in other B<sub>12</sub>-dependent enzymes. In (a), the results of a relaxed scan in gas phase along glycosidic bond, the O<sub>4</sub>–C<sub>1</sub>–N<sub>9</sub>–C<sub>8</sub> dihedral angle, of an isolated Ado $\cdot$  moiety. The scan uncovers several free energy minimum structures:  $\phi$  of 48°, –11°, and –110°. All energies (M06/6-31G(d)) are relative to an arbitrarily chosen origin, an orientation of Ado $\cdot$  taken from the QM/MM simulations following AdoCbl bond cleavage (an averaged value of  $\phi$  of  $115^\circ \pm 8.9^\circ$ ). Performing a geometry optimization of Ado $\cdot$  from this bound state gains nearly 5 kcal mol<sup>-1</sup> of energy via the rotation of  $\phi$  from  $115^\circ$  to  $48^\circ$  (indicated by the dashed gray line connecting these two points). In (b), the  $\phi$  values taken from various B<sub>12</sub>-dependent enzymes, plotted as a function of AdoCbl bond length. The gray points represent the average dihedral value for each cluster. When bound to Co(III), the value of  $\phi$  is  $50$ – $80^\circ$  larger than it is in the unbound state. As previously suggested,<sup>21</sup> the global minimum structure in the gas phase ( $\phi = -11^\circ$ ) is stabilized by an intramolecular hydrogen bond between H–O<sub>2</sub> and N<sub>3</sub>, which is not observed in the condensed phase.

conformation ( $\phi = 47^\circ \pm 23.5^\circ$ ), within 5 ps after homolysis at a Co–C bond length of 4.6 Å. This state is stable during 10 ps and is consistent with crystal structures in which AdoCbl is in the unbound state<sup>11,22</sup> (see Supplementary Figure 2 and Supplementary Table 2, Supporting Information).

**Intramolecular Stabilization Mechanism of 5'-Deoxyadenosyl Radical.** Our findings suggest that the rotation of  $\phi$  from  $>90^\circ$  to  $\sim 47^\circ$  fulfills two distinct purposes, which we describe below: (i) it stabilizes the radical intermediate and thereby prevents deleterious side reactions from occurring, and (ii) it is one of the factors shifting equilibrium in favor of radical propagation instead of recombination. To address the first point, this conformational change brings the C<sub>5'</sub> radical center within 3 Å of the hydrogen atom (H<sub>8</sub>) on the C<sub>8</sub> atom. This stable conformer supports the previous suggestion that intramolecular stabilization of Ado $\cdot$  yields a configuration similar to the 8,5'-cyclic structure.<sup>24</sup> The formation of the 8,5'-cyclic structure is reported to be strongly exothermic (by 10–20 kcal mol<sup>-1</sup>)<sup>21</sup> with the lowest transition state lying at about 10 kcal mol<sup>-1</sup>. We find the barrier for abstraction of the H<sub>8</sub>

atom to be kinetically noncompetitive to the native reaction ( $4.0 \pm 0.5$  kcal mol<sup>-1</sup> higher than the native hydrogen abstraction reaction, see Supplementary Figure 4, Supporting Information). Thus, rotation of  $\phi$  leads to a stable conformation of Ado $\cdot$ , which secures its reactivity during its journey to the substrate. These findings naturally lead to the question: does the enzyme guide this conformational change or simply host it?

To answer this question, we carried out gas phase calculations to discern whether or not the rotation of  $\phi$  is favored in the absence of the protein environment. Starting configurations of Ado $\cdot$  were taken from the QM/MM simulations and from various crystal structures in both the “bound” ( $\phi > 90^\circ$ ) and “unbound” ( $\phi = 45$ – $55^\circ$ ) states. Geometry optimizations converge to a single, stationary minimum ( $\phi = 48^\circ$ ) with the adenosine base in a similar orientation (*anti*) to that of the “unbound” Ado $\cdot$  in the protein environment. A scan of  $\phi$  reveals additional minimum energy conformers, consistent with those found in a previous computational study,<sup>21</sup> corresponding to stationary minima with  $\phi$  angles of  $48^\circ$ ,  $-11^\circ$ , and  $-110^\circ$  (–4.8, –13.6, and –7.0 kcal mol<sup>-1</sup> lower in energy than  $\phi > 90^\circ$ ; see Figure 3a and Supplementary Figure 5 and Supplementary Table 3, Supporting Information). Our findings are consistent with those from another study,<sup>19</sup> which suggest that the rotation of  $\phi$  from its original position ( $\phi > 90^\circ$  and parallel to the corrinoid), stabilizes Ado $\cdot$  by nearly 5 kcal mol<sup>-1</sup> (see Figure 3a). These findings are in agreement with Ado $\cdot$  conformational changes in other AdoCbl-dependent isomerases,<sup>21</sup> which may accompany and possibly facilitate the scission of the AdoCbl bond. In comparison to these gas phase calculations, we computed a free energy estimate for the syn to anti transition ( $\phi$  from  $\sim 47^\circ$  to  $90^\circ$ ) in the unbound state and in the enzyme environment to be 8 kcal mol<sup>-1</sup>.

Therefore, the results from gas phase calculations indicate that this conformational change is intrinsic to Ado $\cdot$  and independent of the enzyme environment. Indeed, a chain of mostly small and hydrophobic residues (L374, P375, Y89, A90, G91, V115, and A116) lines the cavity surrounding the adenosine base to allocate enough space for this rotation of  $\phi$  to occur. Hydrogen bonding with the base occurs only with the backbone atoms of the protein and is readily transferred from G91 in the *syn* configuration to A116 in the *anti* configuration. Evidence from crystal structures of various other B<sub>12</sub>-dependent enzymes lends further support to the idea that the family provides an environment that allows for unobstructed rotation of  $\phi$  to occur. Within the B<sub>12</sub>-dependent family of enzymes, the value of  $\phi$  in different crystal structures corresponds to the values of “bound” and “unbound” Ado $\cdot$  that we observe in MCM ( $\phi \geq 90^\circ$ ,  $\sim 47^\circ$ , and  $-110$  to  $-150^\circ$  in Figure 3b). Looking at the active sites among this family of enzymes, we find that many are lined with small, hydrophobic residues similar to those found in the vicinity of the adenine base in MCM (1b in Figure 2). Having available space in the active site as well as nonpolar and uncharged residues in the vicinity of Ado $\cdot$  may be two important factors enabling this conformational change.

Apart from these hydrophobic interactions, a polar contact stabilizes Ado $\cdot$  in the form of hydrogen bonding interactions between the O<sub>4</sub> atom of Ado $\cdot$  and a nearby residue, Y89. This so-called “aromatic wedge” residue is ascribed to accelerate AdoCbl bond homolysis and has been proposed to directly influence the formation of the radical species.<sup>5,12</sup> Our

simulations reveal that a flexible movement of Y89 accommodates the rotation of  $\phi$  from  $>90^\circ$  to  $48^\circ$  and then allows for a strong hydrogen bond to form with Ado $\cdot$  (1.6 Å, see Supplementary Video 1, Supporting Information). This observed interaction between Y89 and Ado $\cdot$  may also explain why recombination of the AdoCbl bond is favored in the Y89F mutant despite minimal differences in structure between mutant and wild-type enzyme.<sup>5</sup>

**Conformational Changes That Accompany Hydrogen Abstraction.** After cleavage of the Co–C bond has taken place, the diffusion of Ado $\cdot$  from the cavity together with the rotation of  $\phi$  ( $>90^\circ$  to  $17\text{--}47^\circ$ ) guides the  $C_5'$  radical center to a location within 4 Å of the substrate—an ideal starting platform to initiate the hydrogen abstraction reaction. At this site, Ado $\cdot$  is positioned among several charged and polar amino acids situated 7–10 Å from cobalamin center (E247, Y243, Q330, and N366). Hydrogen bonding interactions between these residues and the  $O_2'$ ,  $O_3'$  atoms and their respective hydrogen atoms of the ribose moiety secure its positioning at this site in the protein. These findings are consistent with crystallographic structures that capture AdoCbl in the “un-bound” state (4REQ).<sup>22</sup> However, the proper positioning of Ado $\cdot$  alone does not prevent the radical intermediate from undergoing deleterious side reactions with the substrate. Because hydrogen abstraction from an unactivated primary carbon atom requires a high level of specificity, side reactions with lower energy barriers and/or products that are thermodynamically favored are highly competitive. For example, Ado $\cdot$  must be selective enough to discern a primary hydrogen atom ( $H_{1^\circ}$ ) from the tertiary hydrogen atom ( $H_{3^\circ}$ ) bound to the subsequent carbon atom on the substrate (Figure 4a). The latter leads to a more thermodynamically stable radical intermediate and would not induce a 1,2-rearrangement reaction.

How the enzyme manipulates and controls the transient Ado $\cdot$  moiety was investigated using QM/MM simulations. Starting from the cleaved structure, we investigated the hydrogen abstraction reaction using the distance between the  $C_5'$  atom and the nearest  $H_{1^\circ}$  atom on the substrate as reaction coordinate. The free energy barrier for abstraction is  $11.3 \pm 0.3$  kcal mol $^{-1}$ , in agreement with other computational studies.<sup>15,16</sup> However, the rate of the hydrogen transfer can be expected to increase by at least 1 or 2 orders of magnitude due to quantum tunneling effects.<sup>17,18</sup> We also investigated the barrier of abstraction in the absence of the rotation of  $\phi$  in Ado $\cdot$  and found that, without this conformational change, the barrier increases by  $6.0 \pm 1.0$  kcal mol $^{-1}$  (see Supplementary Figure 4, Supporting Information). These findings further suggest that the intramolecular stabilization mechanism of Ado $\cdot$  is a required transformation that precedes hydrogen abstraction and apparently sets the stage for other crucial conformational changes to take place.

During hydrogen abstraction, a second, key conformational change in Ado $\cdot$  preempts the transfer of the radical to the substrate. At a  $C_5'\cdots H_{1^\circ}$  bond distance of 1.9 Å, we observe a spontaneous change in the puckering of the ribose moiety from  $C_3'$ -endo (2a in Figure 2) to  $C_2'$ -endo (2b in Figure 2 and Supplementary Figure 6, Supporting Information). At this point in the reaction, the  $C_5'$  atom and the  $H_8$  atom approach an interatomic distance of 2.7 Å before the conformational change to  $C_2'$ -endo occurs. Just before this transition takes place, the adenosine base toggles between  $H_{1^\circ}$  and the  $C_5'$  atom (see 2b in Figure 2), which brings the  $C_5'$  radical center into a position

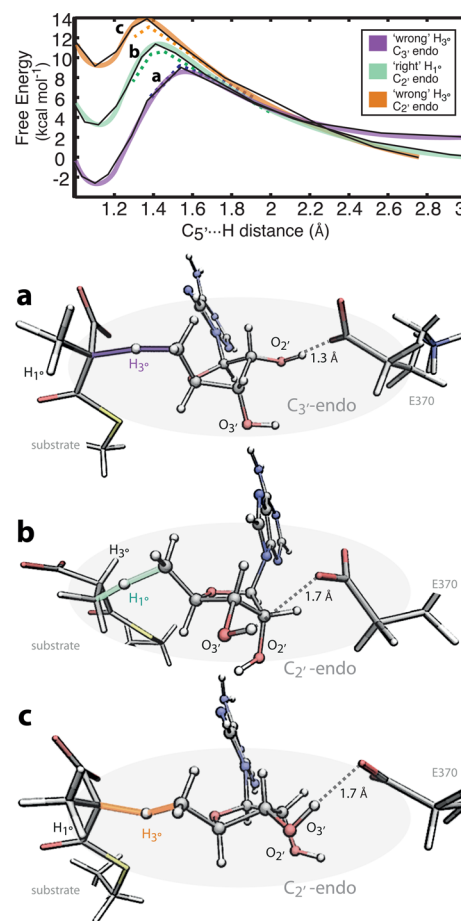


**Figure 4.** Preventing unproductive side reactions. Using QM/MM simulations, the free energy profiles for the native hydrogen ( $H_{1^\circ}$ ) abstraction and a deleterious side reaction, the abstraction of the tertiary hydrogen atom ( $H_{3^\circ}$ ) on the subsequent carbon atom, are shown at the top. In the native reaction mechanism, shown in green and labeled **b**, the shift in ribose puckering of the Ado $\cdot$  moiety from  $C_3'$ -endo to  $C_2'$ -endo occurs spontaneously during the hydrogen abstraction step and is accommodated by MCM via a nearby glutamate residue, E370. In the absence of this conformational change, the Ado $\cdot$  remains in the  $C_3'$ -endo conformation, and the abstraction of the “wrong” hydrogen atom (in this case,  $H_{3^\circ}$ ) is thermodynamically and kinetically favored over the native reaction (see purple curve, labeled **a**). In contrast, abstraction of the same hydrogen,  $H_{3^\circ}$ , is no longer favored if Ado $\cdot$  adopts the  $C_2'$ -endo conformation (see orange curve labeled **c**).

that is equidistant from both the  $H_{1^\circ}$  and the  $H_8$  atoms (Figure 4b and Supplementary Figures 6 and 7, Supporting Information). The transition to the  $C_2'$ -endo conformer radically manipulates and constrains the geometry of Ado $\cdot$ , forcing the  $C_5'$  atom to orient away from the  $H_8$  atom and toward  $H_{1^\circ}$ . This spontaneous transitioning between states is consistent with gas phase calculations, which indicate that the  $C_2'$ -endo conformer is only slightly lower in energy than its counterpart ( $1.5$  kcal mol $^{-1}$ ). These two distinct conformations of the ribose moiety of Ado $\cdot$  are also in agreement with the experimentally observed “ribose pseudorotation” in the crystallographic structure of glutamate mutase.<sup>8</sup>

**A Mechanism to Control the Selectivity of 5'-Deoxyadenosyl Radical.** Previous findings suggest that the  $C_2'$ -endo conformer rigidly confines the trajectory of the  $C_5'$  atom and directs the radical center toward the hydrogen atom



to be abstracted.<sup>8</sup> Our QM/MM simulations provide further evidence of this proposal and present additional details that clarify why this conformational change is crucial in upholding the selectivity of Ado $\cdot$ . We find that specific enzymatic interventions have evolved to prevent certain configurations of Ado $\cdot$  that might lead to erroneous side reactions with the substrate. One such configuration that is blocked by the enzyme during hydrogen abstraction is that of the C<sub>3</sub>-endo conformer of Ado $\cdot$ . Without the change in ribose puckering to the C<sub>2</sub>-endo conformer, the abstraction of the H<sub>3</sub> $\alpha$  atom from the substrate is found to be strongly competitive with a barrier for abstraction of  $9.0 \pm 0.2$  kcal mol<sup>-1</sup> (Figure 4a). This unproductive alternative would be both kinetically and thermodynamically favored over the native abstraction reaction.

Fortunately, the enzyme is actively involved at this point in the reaction to prevent such mistakes from occurring. Evidently, the enzyme is “spring-loaded” in a conformation in which functional groups are positioned to accommodate one particular conformer, depending on the distinct stage of the catalytic cycle. For the initial C<sub>3</sub>-endo geometry, Y243 and Q330 hydrogen bond to the H–O<sub>3'</sub> and O<sub>3'</sub> atoms of the ribose moiety. Upon transitioning to C<sub>2</sub>-endo geometry, the enzyme provides the H–O<sub>3'</sub> atom with a substitute hydrogen bonding partner, E370, capable of accommodating its newly equatorial position (Figure 4b, Supplementary Figure 8 and Supplementary Video 2, Supporting Information). This change effectively constrains the C<sub>5'</sub> radical center and reduces the likelihood of Ado $\cdot$  abstracting the “wrong” hydrogen atom. By reinforcing the conformational switch of C<sub>3</sub>-endo to C<sub>2</sub>-endo, the barrier of abstraction of the H<sub>3</sub> $\alpha$  atom increases by 4 kcal mol<sup>-1</sup> (to  $14.0 \pm 0.8$  kcal mol<sup>-1</sup>) and is no longer competitive to the native abstraction of the H<sub>1</sub> $\alpha$  atom (Figure 4c).

It has recently been shown that mutation of this conserved glutamate residue, denoted E370 in *P. shermanii*, to aspartate in OAM (E338D) and human MCM protein (E338D) generates mutants with 380- and 60-fold reductions in catalytic turnover<sup>30</sup> (see Supplementary Figure 9, Supporting Information for a comparison of active site residues). To be sure that the same behavior is also observed for the system studied in this contribution, site-directed mutagenesis experiments were carried out for the enzyme present in *P. shermanii*. We find that the mutation E370D reduces the catalytic activity by 50-fold relative to the wild-type MCM activity, which is in good agreement to the above studies (see Supplementary Figures 10 and 11, Supporting Information). Taken together, these findings indicate that the mutation of this conserved residue drastically reduces catalytic turnover in the mutant enzyme. It has been proposed that the glutamate residue plays a role in controlling the initial generation of the radical species.<sup>30</sup> However, on the basis of our computational findings for this mutant (Supplementary Figure 12, Supporting Information) as well as a detailed comparison of various crystallographic structures (Supplementary Table 2, Supporting Information), it seems more likely that, in the case of MCM, the main role of this residue is in the control of the hydrogen abstraction step.

**Activating and Deactivating the Mechanochemical Switch.** Our findings suggest that a mechanochemical switch is activated or deactivated at distinct stages of the catalytic cycle to control the highly reactive nature of Ado $\cdot$ . During the first catalytic step, spontaneous changes in the conformation of Ado $\cdot$  accompany cleavage via a rotation of  $\phi$  from  $>90^\circ$  to  $47^\circ$ . We suggest that this conformational change favors the forward propagation of radical species in two distinct ways: (i) the

stability of Ado $\cdot$  increases by means of favorable intramolecular interactions, and the formation of a strong hydrogen bond between Ado $\cdot$ :O<sub>4'</sub> and Y89 and (ii) sets the stage for other crucial conformational changes in Ado to take place during the hydrogen abstraction step. Thus, at this stage in the catalytic cycle, the enzyme is an exemplar of a passive control element (i.e., the switch is turned “off”) and provides a conducive environment for the intramolecular stabilization of Ado $\cdot$  to take place. The fact that the enzyme uses a “preprogrammed” technique to control Ado $\cdot$  is evidenced by the spacious hydrophobic cavity available to Ado $\cdot$  upon diffusion out from its binding site. This hydrophobic cavity permits the radical to adopt an unreactive conformation while it diffuses through the protein.

In contrast, during the second step of the catalytic cycle, the enzyme acts as an active control element, in which the mechanochemical switch is turned “on”. At this point in the cycle, the control of Ado $\cdot$  involves direct manipulation of the ribose geometry. Changes in puckering from C<sub>3</sub>-endo to C<sub>2</sub>-endo are induced by nearby polar and charged residues, which effectively transfer hydrogen bonding interactions from the H–O<sub>3'</sub> atom in an axial position to its equatorial counterpart. Unlike the first step, the function of this second conformational change is less about the stabilization of Ado $\cdot$  and more about manipulating the orientation and steric properties of the radical species to prevent deleterious side reactions. We have shown that the abstraction of a tertiary hydrogen atom (rather than the proper primary hydrogen atom) of the substrate can be avoided via this conformational change.

## CONCLUSIONS

Dealing with radical intermediates is an extremely demanding task, requiring the assemblage of different control tactics. In the case of AdoCbl-dependent enzymes, nature has found a way to utilize an exceptionally effective mechanochemical switch, which is activated and deactivated at specific stages during the catalytic cycle to gain control of reactive intermediates. Depending on the intrinsic or extrinsic factors during the catalytic cycle, the switch can either be turned “off” to utilize internal strain and stored energy via spontaneous conformational changes in Ado $\cdot$  or “on” to utilize the enzyme environment as the driving force for propelling forward a desired chemical task. This mechanochemical switch illustrates one way in which enzymes attain selectivity of extremely chemically challenging reactions.

## ASSOCIATED CONTENT

### Supporting Information

Further details of the procedures used to model MCM, perform CPMD simulations, and the experimental details. This material is available free of charge via the Internet at <http://pubs.acs.org/>.

## AUTHOR INFORMATION

### Corresponding Author

\*E-mail: [ursula.roethlisberger@epfl.ch](mailto:ursula.roethlisberger@epfl.ch). Phone: +41 (0)21 693 0321. Fax: +41 (0)21 693 0320.

### Funding

Funding resources include the Swiss National Science Foundation (Grant 200020-146645), the National Institutes of Health (Grant DK061666).

## Notes

The authors declare no competing financial interest.

## ACKNOWLEDGMENTS

The authors gratefully acknowledge support from the Swiss National Science Foundation award 200020-146645, the IT domain (DIT) of EPFL, the Swiss National Computing Center (CSCS), and BlueGene for computing resources. In addition, the authors thank Helena Martin for contributing artwork for the graphical abstract and Professor Hatzimanikatis for early support on this project.

## ABBREVIATIONS USED

B<sub>12</sub>, vitamin B<sub>12</sub>; Ado·, 5'-deoxyadenosyl radical; MCM, methyl malonyl-CoA mutase; QMMM, quantum mechanical/molecular mechanical; AdoCbl, 5'-deoxyadenosyl-cobalamin; AdoB<sub>12</sub>, adenosyl-B<sub>12</sub>; GM, glutamate mutase; OAM, ornithine 4,5-aminomutase; MD, molecular dynamics; CPMD, Car-Parrinello molecular dynamics; BOMD, Born-Oppenheimer molecular dynamics; DFT, density functional theory

## REFERENCES

- (1) R    , J. (1990) Enzymic Reaction Selectivity by Negative Catalysis or How Do Enzymes Deal with Highly Reactive Intermediates? *Angew. Chem. Int. Ed.* 29, 355–361.
- (2) Banerjee, R., and Ragsdale, S. W. (2003) The Many Faces of Vitamin B<sub>12</sub>: Catalysis by Cobalamin-Dependent Enzymes. *Annu. Rev. Biochem.* 72, 209–247.
- (3) Hay, B. P., and Finke, R. G. (1986) Thermolysis of the cobalt-carbon bond of adenosylcobalamin. 2. Products, kinetics, and cobalt-carbon bond dissociation energy in aqueous solution. *J. Am. Chem. Soc.* 108, 4820–4829.
- (4) Hay, B. P., and Finke, R. G. (1987) Thermolysis of the Co-C bond in adenosylcobalamin. 3. Quantification of the axial base effect in adenosylcobalamin by the synthesis and thermolysis of axial base-free adenosylcobinamide. Insights into the energetics of enzyme-assisted cobalt-carbon bond homolysis. *J. Am. Chem. Soc.* 109, 8012–8018.
- (5) Vlasie, M., and Banerjee, R. (1998) Tyrosine 89 Accelerates Co-Carbon Bond Homolysis in Methylmalonyl-CoA Mutase. *J. Am. Chem. Soc.* 120, 5431–5435.
- (6) Pang, J., Li, X., Morokuma, K., Scrutton, N., and Sutcliffe, M. J. (2012) Large-scale Domain Conformational Change is Coupled to the Activation of the Co-C Bond in the B<sub>12</sub>-Dependent Enzyme Ornithine 4,5-Aminomutase: A Computational Study. *J. Am. Chem. Soc.* 134, 2367–2377.
- (7) Masuda, J., Shibata, N., Morimoto, Y., Toraya, T., and Yasuoka, N. (2000) How a protein generates a catalytic radical from coenzyme B<sub>12</sub>: X-ray structure of a diol-dehydratase-adeninylpentylcobalamin complex. *Structure* 8, 775–788.
- (8) Reitzer, R., Gruber, K., and Kratky, C. (2001) Radical Shuttling in a Protein: Ribose Pseudorotation Controls Alkyl-Radical Transfer in the Coenzyme B<sub>12</sub> Dependent Enzyme Glutamate Mutase. *Angew. Chem. Int. Ed.* 40, 3377–3380.
- (9) Bandarian, V., and Reed, G. H. (2002) Analysis of the electron paramagnetic resonance spectrum of a radical intermediate in the coenzyme B<sub>12</sub>-dependent ethanolamine ammonia-lyase catalyzed reaction of S-2-aminopropanol. *Biochemistry* 41, 8580–8588.
- (10) Chowdhury, S., and Banerjee, R. (2000) Thermodynamic and kinetic characterization of Co-C bond homolysis catalyzed by coenzyme B<sub>12</sub>-dependent methylmalonyl-CoA mutase. *Biochemistry* 39, 7998–8006.
- (11) Froese, D. S., Kochan, G., Muniz, J., Wu, X., Gileadi, C., Ugochukwu, E., Krysztofinska, E., Gravel, R. A., Oppermann, U., and Yue, W. W. (2010) Structures of the human GTPase MMAA and vitamin B<sub>12</sub>-dependent methylmalonyl-coa mutase and insight into their complex formation. *J. Biol. Chem.* 285, 38204–38213.

- (12) Thoma, N. H., Meier, T. W., Evans, P. R., and Leadlay, P. F. (2000) Stabilization of Radical Intermediates by an Active-Site Tyrosine Residue in Methylmalonyl-CoA Mutase. *Biochemistry* 37, 14386–14393.
- (13) Kwiecien, R. A., Khavrutski, L. V., Musaev, D. G., Morokuma, K., Banerjee, R., and Paneth, P. (2006) Computational Insights into the Mechanism of Radical Generation in B<sub>12</sub>-Dependent Methylmalonyl-CoA Mutase. *J. Am. Chem. Soc.* 128, 1287–1292.
- (14) Jensen, K. P., and Ryde, U. (2009) Cobalamins uncovered by modern electronic structure calculations. *Coord. Chem. Rev.* 253, 769–778.
- (15) Bucher, D., Sandala, G. M., Durbeej, B., Radom, L., and Smith, D. M. (2012) The Elusive 5'-Deoxyadenosyl Radical in Coenzyme-B<sub>12</sub>-Mediated Reactions. *J. Am. Chem. Soc.* 134, 1591–1599.
- (16) Semialjac, M., and Schwarz, H. (2004) Computational investigation of hydrogen abstraction from 2-aminoethanol by the 1,5-dideoxyribose-5-yl radical: A model study of a reaction occurring in the active site of ethanolamine ammonia lyase. *Chem.—Eur. J.* 10, 2781–2788.
- (17) Dybala-Defratyka, A., Paneth, P., Banerjee, R., and Truhlar, D. J. (1998) Coupling of hydrogenic tunneling to active-site motion in the hydrogen radical transfer catalyzed by a coenzyme B<sub>12</sub>-dependent mutase. *Proc. Nat. Acad. Sci. U.S.A.* 104, 10774–10779.
- (18) Rommel, J. B., Liu, Y., Werner, H.-J., and K      , J. (2012) Role of tunneling in the enzyme glutamate mutase. *J. Phys. Chem. B* 116, 13682–13689.
- (19) Pang, J., Li, X., Morokuma, K., Scrutton, N. S., and Sutcliffe, M. J. (2012) Large-Scale Domain Conformational Change Is Coupled to the Activation of the Co-C Bond in the B<sub>12</sub>-Dependent Enzyme Ornithine 4, 5-Aminomutase: A Computational Study. *J. Am. Chem. Soc.* 134, 2367–2377.
- (20) Marsh, E. N. G., and Drennan, C. L. (2001) Adenosylcobalamin-dependent isomerases: new insights into structure and mechanism. *Curr. Opin. Chem. Biol.* 5, 499–505.
- (21) Khoroshun, D. V., Warncke, K., Ke, S.-C., Musaev, D. G., and Morokuma, K. (2003) Internal Degrees of Freedom, Structural Motifs, and Conformational Energetics of the 5'-Deoxyadenosyl Radical: Implications for Function in Adenosylcobalamin-Dependent Enzymes. A Computational Study. *J. Am. Chem. Soc.* 125, 570–579.
- (22) Mancia, F., and Evans, P. R. (1998) Conformational changes on substrate binding to methylmalonyl CoA mutase and new insights into the free radical mechanism. *Structure* 6, 711–720.
- (23) Pullman, B., and Saran, A. (1976) Quantum-Mechanical Studies on the Conformation of Nucleic Acids and Their Constituents Progress in Nucleic Acid Research and Molecular Biology. *Prog. Nucleic Acid Res. Mol. Biol.* 18, 215–325.
- (24) Sando, G. N., Blakley, R. L., Hogenkamp, H. P. C., and Hoffman, P. J. (1975) Studies on the Mechanism of Adenosylcobalamin-dependent Ribonucleotide Reduction by the Use of Analogs of the Coenzyme. *J. Biol. Chem.* 250, 8774–8779.
- (25) Shelton, K. R., and Clark, K. M. (1967) A Proton Exchange between Purines and Water and Its Application to Biochemistry. *Biochemistry* 6, 2735–2739.
- (26) Buckel, W., Kratky, C., and Golding, B. T. (2006) Stabilisation of methylene radicals by cob (II) alamin in coenzyme B<sub>12</sub> dependent mutases. *Chem.—Eur. J.* 12, 352–362.
- (27) Friedrich, P., Baisch, U., Harrington, R. W., Lyatuu, F., Zhou, K., Zelder, F., McFarlane, W., Buckel, W., and Golding, B. T. (2012) Experimental Study of Hydrogen Bonding Potentially Stabilizing the 5'-Deoxyadenosyl Radical from Coenzyme B<sub>12</sub>. *Chem.—Eur. J.* 18, 16114–16122.
- (28) Durbeej, B., Sandala, G. M., Bucher, D., Smith, D. M., and Radom, L. (2009) On the Importance of Ribose Orientation in the Substrate Activation of the Coenzyme B<sub>12</sub>-Dependent Mutases. *Chem.—Eur. J.* 15, 8578–8585.
- (29) Buckel, W., Friederich, P., and Golding, B. T. (2012) Hydrogen bonds guide the short-lived 5'-deoxyadenosyl radical to the place of action. *Angew. Chem., Int. Ed. Engl.* 51, 9974–9976.



- (30) Makins, C., Pickering, A. V., Mariani, C., and Wolthers, K. R. (2013) Mutagenesis of a Conserved Glutamate Reveals the Contribution of Electrostatic Energy to Adenosylcobalamin Co-C Bond Homolysis in Ornithine 4,5-Aminomutase and Methylmalonyl-CoA Mutase. *Biochemistry* 52, 878–888.
- (31) Case, D. A. et al. (2008) *AMBER 10*, University of California, San Francisco, CA.
- (32) Wang, J., Cieplak, P., and Kollman, P. A. (2000) How Well Does a Restrained Electrostatic Potential (RESP) Model Perform in Calculating Conformational Energies of Organic and Biological Molecules? *J. Comput. Chem.* 21, 1049–1074.
- (33) Marques, H. M., Ngoma, B., Egan, T. J., and Brown, K. L. (2001) Parameters for the amber force field for the molecular mechanics modeling of the cobalt corrinoids. *J. Mol. Struct.* 561, 71–91.
- (34) Feller, S. E., Zhang, Y., Pastor, R. W., and Brooks, B. R. (1995) Constant pressure molecular dynamics simulation: The Langevin piston method. *J. Chem. Phys.* 103, 4613–4621.
- (35) Martyna, G. J., Tobias, D. J., and Klein, M. L. (1994) Constant pressure molecular dynamics algorithms. *J. Chem. Phys.* 101, 4177–4189.
- (36) Laio, A., VandeVondele, J., and Rothlisberger, U. (2002) A Hamiltonian electrostatic coupling scheme for hybrid Car-Parrinello molecular dynamics simulations. *J. Chem. Phys.* 116, 6941–6948.
- (37) Car, R., and Parrinello, M. (1985) Unified Approach for Molecular Dynamics and Density-Functional Theory. *Phys. Rev. Lett.* 55, 2471–2474.
- (38) Lee, C., Yang, W., and Parr, R. G. (1988) Development of the Colle-Salvetti correlation-energy formula into a functional of the electron density. *Phys. Rev. B* 37, 785–789.
- (39) Becke, A. D. (1988) Density-functional exchange-energy approximation with correct asymptotic behavior. *Phys. Rev. A* 38, 3098–3100.
- (40) Troullier, N., and Martins, J. L. (1991) Efficient pseudopotentials for plane-wave calculations. II. Operators for fast iterative diagonalization. *Phys. Rev. B* 43, 8861–8869.
- (41) von Lilienfeld, O. A., Sebastiani, D., Tavernelli, I., and Rothlisberger, U. (2004) Optimization of Effective Atom Centered Potentials for London Dispersion Forces in Density Functional Theory. *Phys. Rev. Lett.* 93, 153004.
- (42) Jensen, K. P., and Ryde, U. (2003) Theoretical prediction of the Co-C bond strength in cobalamins. *J. Phys. Chem. A* 107, 7539–7545.
- (43) Kumar, N., Alfonso-Prieto, M., Rovira, C., Lodowski, P., Jaworska, M., and Kozłowski, P. M. (2011) Role of the Axial Base in the Modulation of the Cob (I) alamin Electronic Properties: Insight from QM/MM, DFT, and CASSCF Calculations. *J. Comput. Chem.* 7, 1541–1551.
- (44) Alfonso-Prieto, M., Biarnés, X., Kumar, M., Rovira, C., and Kozłowski, P. M. (2010) Reductive Cleavage Mechanism of Co- C Bond in Cobalamin-Dependent Methionine Synthase. *J. Phys. Chem. B* 114, 12965–12971.
- (45) Rovira, C., Biarnés, X., and Kunc, K. (2004) Structure-energy relations in methylcobalamin with and without bound axial base. *Inorg. Chem.* 43, 6628–6632.
- (46) von Lilienfeld, O. A., Tavernelli, I., Hutter, J., and Rothlisberger, U. (1988) Variational Optimization of Effective Atom Centered Potentials for Arbitrary Properties. *J. Chem. Phys.* 122, 014113.
- (47) Kurmaev, E. Z., Moewes, A., Ouyang, L., Randaccio, L., Rulis, P., Ching, W. Y., Bach, M., and Neumann, M. (2003) The electronic structure and chemical bonding of vitamin B12. *Europhys. Lett.* 62, 582.
- (48) Martyna, G. J., and Tuckerman, M. E. (1999) A reciprocal space based method for treating long range interactions in ab initio and force-field-based calculations in clusters. *J. Chem. Phys.* 2810–2821.
- (49) Sprik, M., and Ciccotti, G. (1998) Free energy from constrained molecular dynamics. *J. Chem. Phys.* 109, 7737–7744.
- (50) Frisch, M. J. et al. (2009) *Gaussian 09*, Gaussian, Inc., Wallingford, CT.
- (51) Warren, W. J., Ditchfield, R., and Pople, J. A. (1972) Self-consistent molecular orbital methods. XII. Further extensions of gaussian-type basis sets for use in molecular orbital studies of organic molecules. *J. Chem. Phys.* 56, 2257.
- (52) Brooks, A. J., Vlasie, M., Banerjee, R., and Brunold, T. C. (2004) Spectroscopic and computational studies on the adenosylcobalamin-dependent methylmalonyl-CoA mutase: evaluation of enzymatic contributions to Co-C bond activation in the Co3+ ground state. *J. Am. Chem. Soc.* 270, 8167–8180.
- (53) Padmakumar, R., and Banerjee, R. J. (1995) Evidence from electron paramagnetic resonance spectroscopy of the participation of radical intermediates in the reaction catalyzed by methylmalonyl-coenzyme A mutase. *J. Biol. Chem.* 270, 9295–9300.
- (54) Froese, D. S., Kochan, G., Muniz, J., Wu, X., Gileadi, C., Ugochukwu, E., Krysztofinska, E., Gravel, R. A., Oppermann, U., and Yue, W. W. (2010) Structures of the human GTPase MMAA and vitamin B12-dependent methylmalonyl-CoA mutase and insight into their complex formation. *J. Biol. Chem.* 285, 38204–38213.
- (55) Wolthers, K. R., Levy, C., Scrutton, N. S., and Leys, D. (2010) Large-scale domain dynamics and adenosylcobalamin reorientation orchestrate radical catalysis in ornithine 4,5-aminomutase. *J. Biol. Chem.* 285, 13942–13950.